Research on Engineering Structures & Materials
www.jresm.org
Research Group

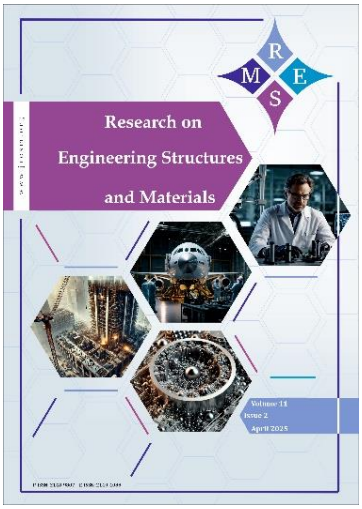

Improved PGA and PGV estimation in soft soils for earthquake engineering applications

Aicha Rouabeh, Issam Aouari, Baizid Benahmed, Mehmet Palanci

Online Publication Date: 30 June 2025

URL: http://www.jresm.org/archive/resm2025-857ea0429rs.html
DOI: http://dx.doi.org/10.17515/resm2025-857ea0429rs

Journal Abbreviation: *Res. Eng. Struct. Mater.*

To cite this article
Rouabeh A, Aouari I, Benahmed B, Palanci M. Improved PGA and PGV estimation in soft soils for earthquake engineering applications. *Res. Eng. Struct. Mater.*, 2025; 11(6): 3167-3186.

Research on Engineering Structures & Materials
www.jresm.org
MIM Research Group

Research Article

Improved PGA and PGV estimation in soft soils for earthquake engineering applications

Aicha Rouabeh [*,1,a], Issam Aouari [1,b], Baizid Benahmed [2,c], Mehmet Palanci [3,d]

[1]*Department of Civil Engineering, Faculty of Applied Sciences, University of Bouira, Bouira, Algeria*
[2]*Development Laboratory in Mechanics and Materials, Ziane Achour University, Djelfa, Algeria*
[3]*Department of Civil Engineering, Istanbul Arel University, Istanbul, Turkiye*

Article Info

Article History:

Received 29 Apr 2025

Accepted 23 June 2025

Keywords:

Peak ground acceleration;
Peak ground velocity;
Soft soils;
Seismic attenuation;
NGA-West2;
Engineering strong motion

Abstract

Soil characteristics play a pivotal role in seismic risk assessment and earthquake-resistant design, with softer soils exhibiting significant ground motion amplification that elevates structural vulnerability. Construction on soft soil sites presents engineering challenges, as seismic wave propagation significantly alters signal characteristics between the source and the site. This study focuses on two critical engineering parameters—Peak Ground Acceleration (PGA) and Peak Ground Velocity (PGV)—developing site-specific predictive models for soft soil conditions (V_{s30} = 180–360 m/s). Utilizing 4,328 records from the PEER NGA-West2 database and 2,462 records from the Engineering Strong Motion (ESM) database, we derive magnitude- and distance-dependent attenuation relationships through nonlinear regression analysis. The models incorporate key variables: moment magnitude (M_w), epicentral distance ($EpiD$), and shear-wave velocity (V_{s30}). The PGA model exhibits accelerated attenuation at short distances compared to conventional models (e.g., Boore et al. 1993), while converging with Campbell (1981) at larger distances. For PGV, the formulation effectively captures intermediate-frequency amplification, addressing systematic underprediction by Joyner & Boore (1988) and overprediction by volcanic-region models (e.g., Tusa & Langer 2016). These advancements provide engineers with optimized tools for soft soil seismic design, directly addressing liquefaction risks, resonance effects, and structural performance.

1. Introduction

Earthquakes pose a severe threat to regions near tectonic plate boundaries, where strong seismic activity can devastate buildings and infrastructure, leading to catastrophic collapses and substantial human and economic losses. The 2023 Kahramanmaraş earthquake exemplifies this vulnerability, with over 38,000 collapsed buildings, 55,000 fatalities, and widespread urban destruction—most of which occurred in soft soil zones [1].

Soft soils, characterized by fine-grained composition, high moisture content, and low shear strength, present critical challenges for geotechnical and structural engineering. These soils are prevalent in coastal seismic hotspots, including Indonesia, the Philippines, Mexico, India, and China. Under static conditions, structures on soft soils often undergo differential settlements, while during earthquakes, they experience amplified ground motion due to two key phenomena:

- Amplification of seismic waves: Soft soils can increase peak acceleration by 1.5–3.5 and extend shaking duration [2,3].

*Corresponding author: a.rouabeh@univ-bouira.dz
[a]orcid.org/0009-0004-8485-523X; [b]orcid.org/0000-0001-6920-4608; [c]orcid.org/0000-0003-4924-0059; [d]orcid.org/0000-0002-9223-5629
DOI: http://dx.doi.org/10.17515/resm2025-857ea0429rs

- Frequency filtering: High-frequency waves attenuate, while low frequencies amplify, lengthening the predominant period of ground motion [2]. This shift can resonate with flexible structures (e.g., high-rises, bridges), exacerbating damage.

Soft soils filter high-frequency seismic waves while amplifying longer-period motions, increasing the dominant period of ground shaking transmitted to structures. This effect can lead to seismic subsidence and reduced earthquake resistance, particularly during large earthquakes [3]. This effect increases stress on buildings and infrastructure, making them more vulnerable to damage. Structures designed without considering this amplification may experience unexpected forces, leading to failure.

Soft ground conditions pose significant geotechnical challenges, particularly for structures built on weak or filled-up soil [4], [5]. Soft soils tend to trap and amplify seismic waves, leading to prolonged shaking durations compared to firmer ground [6]. This effect is especially detrimental to high-rise buildings, bridges, and other flexible structures with longer natural vibration periods. To mitigate these risks, seismic isolation has been explored as a viable solution for buildings founded on soft soil, as demonstrated in a case study of a reinforced concrete (RC) building in Shanghai [7]. Nonlinear time-history analyses of base-isolated RC buildings on soft soil further highlight the complexities involved in seismic design under such conditions [8]. Moreover, nonlinear site response analyses often predict significant shear strain (3–10%) for soft soil sites, resulting in large deformations that can introduce unusual characteristics in surface ground motions [9]. These factors emphasize the need for advanced engineering solutions to enhance structural resilience in seismic-prone regions with soft soil foundations.

In their 2024 book [10], Kramer and Stewart comprehensively summarized key seismic parameters (also termed seismic indicators) and discussed their applications in ground motion analysis. These parameters are widely acknowledged as critical indicators of seismic damage potential. The most widely used parameters include Peak Ground Acceleration (PGA), Peak Ground Velocity (PGV), and Peak Ground Displacement (PGD), alongside the PGV/PGA ratio. Additional significant measures encompass root-mean-square (RMS) values of acceleration, velocity, and displacement; Arias Intensity (Ia); Cumulative Absolute Velocity (CAV); and the Predominant Period (Tp).

Horizontal accelerations are widely employed in seismic design to characterize ground motions, owing to their direct correlation with inertial forces. Indeed, Peak Ground Acceleration (PGA) is particularly critical, as it governs the largest dynamic forces in many structures. PGA serves as a fundamental parameter for the Global Earthquake Seismic Hazard Map [11], which depicts the geographic distribution of PGA values corresponding to a 10% probability of exceedance within 50 years. Additionally, PGA is a key metric for regional seismic risk assessment [12,13].

The peak horizontal velocity (PGV) is another useful parameter for characterization of ground motion amplitude. Since the velocity is less sensitive to the higher-frequency components of the ground motion, the PGV is more likely than the PGA to characterize ground motion amplitude accurately at intermediate frequencies [14]. For structures or facilities that are sensitive to loading in this intermediate-frequency range (e.g., tall or flexible buildings, bridges, etc.). Additionally, Peak Ground Velocity (PGV) sometimes employed for risk map evaluation [15]. PGV plays a role in evaluating soil-structure interaction by determining how seismic waves affect soft soil sites and how the ground motion transfers to structures. It helps predict soil liquefaction potential, which can cause foundation instability. Engineers use PGV as an intensity measure for evaluating structural damage, particularly in non-structural components, which can influence retrofitting decisions [16]. Higher PGV values indicate greater deformation potential, serving as a critical metric for estimating structural and geotechnical damage during earthquakes. This relationship is particularly significant in the design and assessment of pipelines and underground structures, where velocity-based loading governs stability and failure mechanisms [17,18].

Previous studies on predicting earthquake amplitude (PGA) for engineering applications have predominantly neglected the critical role of ground conditions in structural response. As highlighted in prior research, structures situated on soft soil sites exhibit pronounced soil-structure interaction effects, which manifest through four principal mechanisms: (1) modification

of input ground vibrations, (2) alteration of system vibration characteristics, (3) dissipation of radiant energy, and (4) material damping energy. To account for these factors and enhance the reliability of computational evaluations, this study develops a predictive model for Peak Ground Acceleration (PGA) and Peak Ground Velocity (PGV) that explicitly incorporates soft soil conditions.

The primary objective of this study is to develop a novel predictive relationship for Peak Ground Acceleration (PGA) and Peak Ground Velocity (PGV) specifically tailored for soft soil sites, with direct applications in structural engineering design and analysis. To achieve this, we employ advanced statistical methods, particularly nonlinear regression techniques, to establish robust and accurate predictive models for these critical seismic parameters under soft soil conditions.

2. Materials and Methods

The study methodology comprised three main phases: data collection, parameter calculation, and model development. Ground motion records were systematically extracted from two authoritative databases - the Pacific Earthquake Engineering Research Center (PEER NGA-West2) [19] and Engineering Strong-Motion (ESM) [20] - with selection criteria requiring moment magnitude (M_w), epicentral distance ($EpiD$), and soil classification data, specifically targeting soft soil conditions (V_{s30} = 180-360 m/s). This yielded 8,790 quality-controlled records from 875 global earthquakes (324 PEER, and 551 ESM). For consistent orientation-independent intensity measures, PGA and PGV were derived using the Rotated Geometric Mean (RotD50) approach, which calculates the median geometric mean across all possible component rotations (0°-180°). Nonlinear regression techniques were then employed to develop predictive models incorporating M_w, $EpiD$, and V_{s30} as primary variables, with particular attention to capturing soft soil amplification characteristics that existing models often misrepresent. The rigorous methodology ensures reliable attenuation relationships specifically optimized for seismic hazard assessment in soft soil regions. The adopted methodology is presented in the flowchart of Fig. 1.

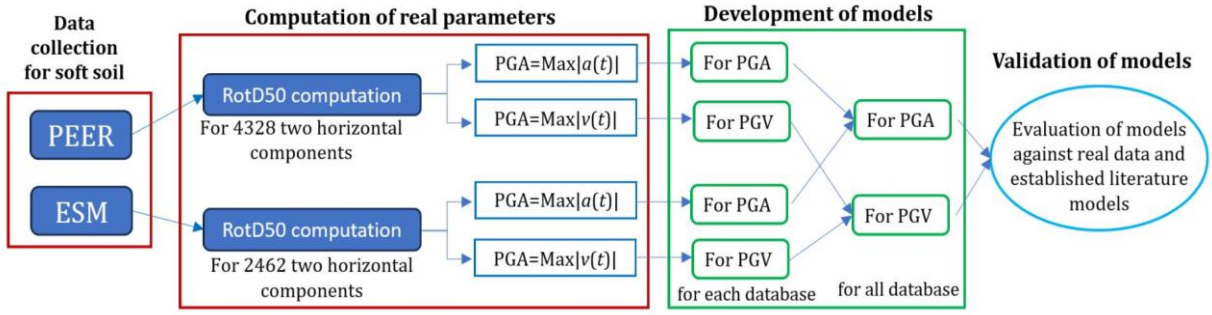

Fig. 1. Flowchart of the adopted methodology

2.1. PGA and PGV Definition

The PGA of a seismic motion component is simply the largest (absolute) value of the acceleration a(t) obtained from the accelerogram. The maximum PGA can be obtained by making the vector sum of two orthogonal components.

$$PGA = Max(|a(t)|) \tag{1}$$

Since velocity, $v(t)$, is the integral of acceleration, a(t), it can be computed as a function of time using numerical integration methods such as the trapezoidal rule. The PGV is defined as the absolute maximum value of $v(t)$.

$$v(t) = \int a(t)dt \;\; hence \; PGV = Max\;(|v(t)|) \tag{2}$$

Fig. 2 compares two different recording stations: Gilroy Array #1, located on a rock site, and Gilroy Array #3, located on a soft soil site, during the Loma Prieta earthquake (magnitude 6.9) on October 17, 1989. From Fig. 2, we observe that at a station located on a rock site (V_{s30} =1428.14 m/sec) at a distance of 9.64 km, the peak acceleration (PGA = 0.485g) and peak velocity (PGV = 32.451 m/sec)

are lower than those recorded at a station on soft soil (V_{s30} = 349.85 m/sec) at a distance of 12.82 km, where PGA = 0.559g and PGV = 36.306 m/sec. These observations confirm the importance of distinguishing between predictive PGA and PGV models for different soil.

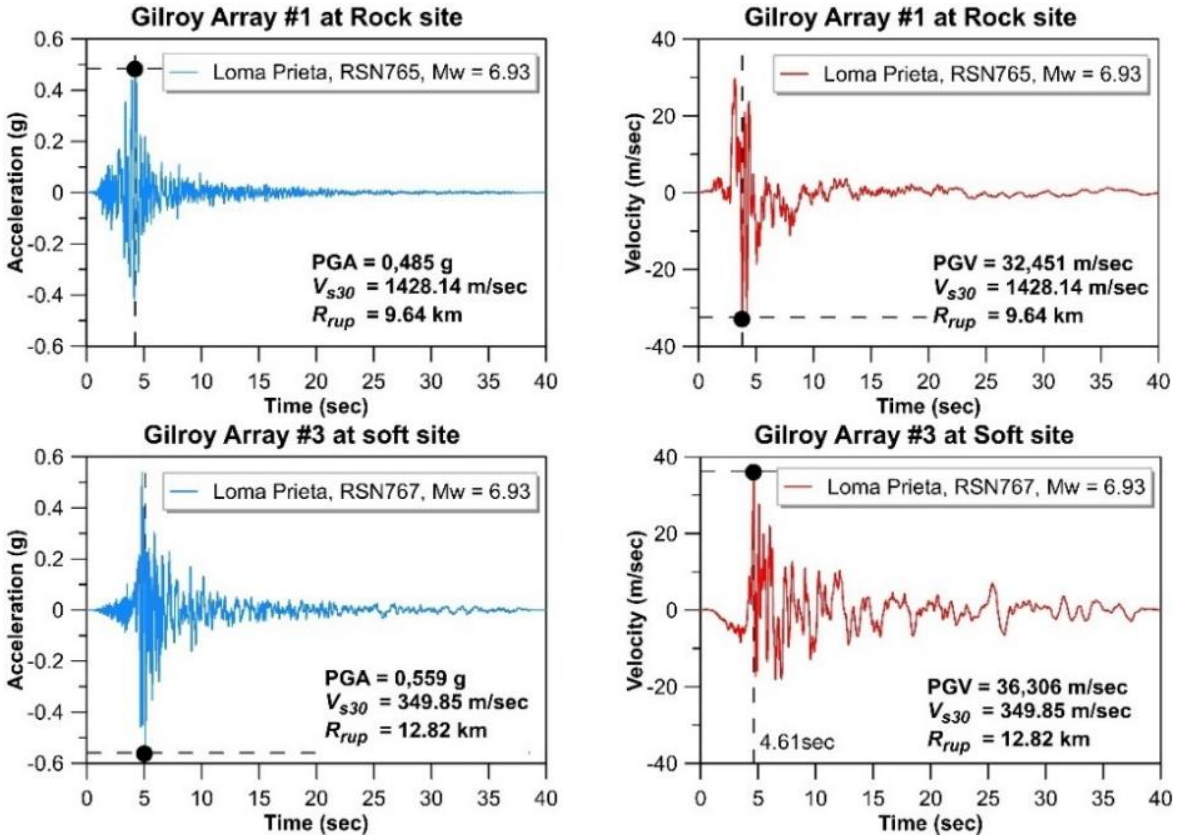

Fig. 2. Acceleration and velocity recordings of the 1989 Loma Prieta earthquake (M_w = 6.93) at two stations: Gilroy Array #1 (rock site) and Gilroy Array #3 (soft soil site)

2.2. Strong Motion Database

This study compiled 6,790 strong-motion records (4,328 from PEER NGA-West2 and 2,462 from ESM) specifically from soft soil sites, defined by shear-wave velocity (V_{s30}) values of 180-360 m/s in accordance with international seismic design standards. The Pacific Earthquake Engineering Research Center's PEER database provided globally distributed records, while the Engineering Strong-Motion (ESM) database contributed European-Mediterranean and Middle Eastern events, ensuring broad geographic representation. All selected records included complete data for moment magnitude (M_w), epicentral distance (*EpiD*), and processed acceleration time histories. The V_{s30} range served as the primary classification parameter, aligning with international seismic design codes (e.g., Eurocode 8, ASCE 7-22). Table 1 summarizes the V_{s30} ranges adopted by major codes and this study's classification thresholds.

Table 1. Soft soil sites class with various codes

Code	Range of V_{s30} (m/s)	Site Classification	Reference
IBC (2006)	180 - 360	D, Stiff and Soft	[21]
NEHRP (2001)	180 - 360	D, Dense to medium soils	[22]
Eurocode 8 (2004)	180 - 360	C, Deep, medium dense or stiff	[23]
UBC (1997)	183 - 366	D, Stiff and Soft	[24]
RPA2024 (2024)	180 - 360	S3, Soft Soil	[25]

Fig. 3 presents the distribution of strong-motion records assembled from the PEER and ESM databases as a function of epicentral distance *EpiD* (a) and shear-wave velocity V_{s30} (b), both plotted against M_w.

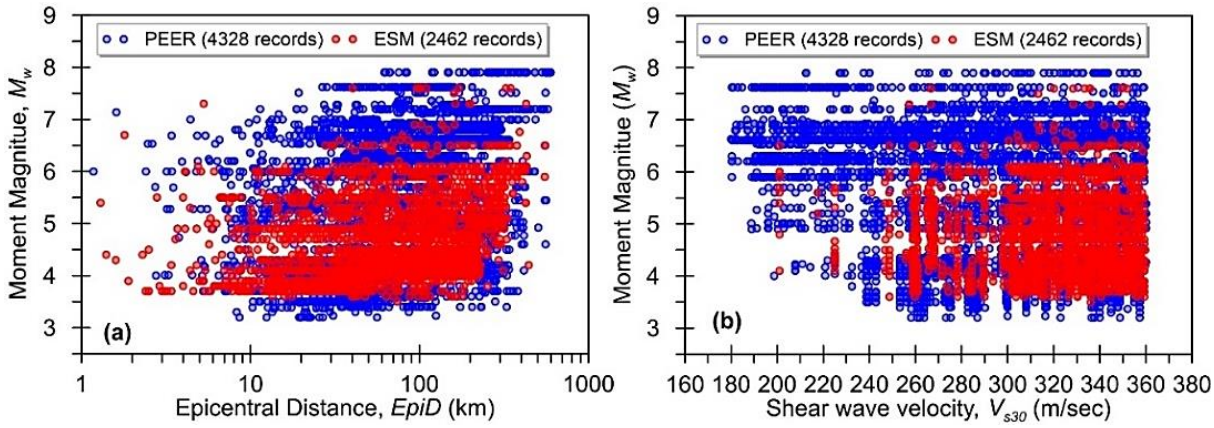

Fig. 3. Distribution of ground-motion records used in the analysis from the PEER (Pacific Earthquake Engineering Research Center) and ESM (Engineering Strong-Motion) databases. (a) Moment magnitude M_w versus epicentral distance (*EpiD*), and (b) Moment magnitude M_w versus average shear-wave velocity in the top 30 meters (V_{s30})

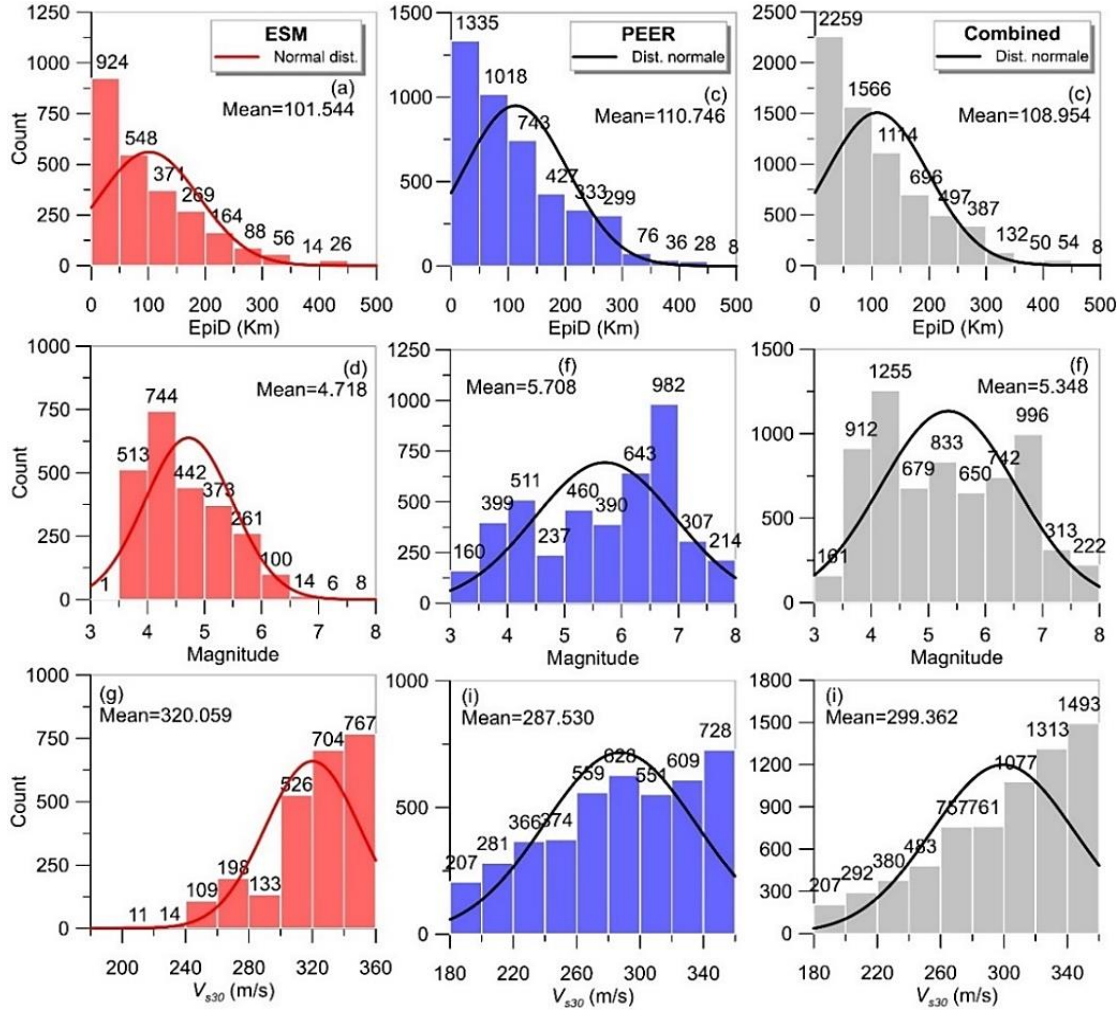

Fig. 4. Distribution of seismic parameters for ground motion records on soft soil sites from the ESM and PEER NGA-West2 databases. Histograms show the distributions of (a–c) epicentral distance (*EpiD*), (d–f) moment magnitude (M_w), and (g–a) average shear-wave velocity in the upper 30 meters (V_{s30})

In panel (a), the PEER database (blue circles) covers a broader range of magnitudes and distances, particularly capturing a significant number of large-magnitude events (M_w > 6) at a wide range of distances (up to several hundred kilometers). The ESM database (red circles), while also spanning

a wide distance range, includes a higher density of records for moderate magnitudes ($M_w \approx 4 - 6$) and distances below 100 km, reflecting its strong regional focus, particularly in Europe. Panel (b) shows the distribution of moment magnitudes against V_{s30}, where the PEER dataset generally exhibits a higher shear-wave velocity range (soft soil sites), while the ESM records cluster around lower V_{s30} values, indicative of softer site conditions. The PEER records extend into very high V_{s30} values (> 350 m/s), whereas the ESM records are more concentrated between 200 and 320 m/s. Overall, the combination of the two datasets ensures a diverse and representative coverage of seismic events, distances, and site conditions, essential for the robust development and validation of ground-motion prediction models.

Fig. 4 illustrates the distribution of key seismic parameters—epicentral distance (*EpiD*), moment magnitude (M_w), and average shear-wave velocity in the upper 30 meters (V_{s30})—for ground motion records on soft soil sites from the ESM and PEER NGA-West2 databases. Subplots (a), (d), and (g) represent the ESM dataset, (b), (e), and (h) represent the PEER dataset, while (c), (f), and (I) show the combined distribution from both sources. Each histogram is overlaid with a fitted normal distribution curve, and the mean values are indicated for reference.

The distributions reveal key differences between the two datasets. The PEER records tend to have slightly larger epicentral distances (mean ≈ 110.7 km) and magnitudes (mean ≈ 5.71) compared to the ESM records (mean *EpiD* ≈ 101.5 km, mean $M_w \approx 4.72$), suggesting broader regional and seismic event coverage. In contrast, the ESM dataset is characterized by higher average V_{s30} values (mean ≈ 320.1 m/s), indicating generally stiffer soft soil site classifications. The combined dataset reflects a balanced integration of both sources, enhancing the representativeness of the seismic input for ground motion analysis on soft soil sites.

3. Results and Discussions

Fig. 5 illustrates the computed Peak Ground Acceleration (PGA, in g) and Peak Ground Velocity (PGV, in cm/s) as functions of moment magnitude (M_w), epicentral distance (*EpiD*), and the average shear-wave velocity in the upper 30 meters (V_{s30}). The analysis is based on ground-motion records from the European Strong-Motion (ESM) and PEER NGA-West2 databases, following the methodology outlined in Section 2.1.

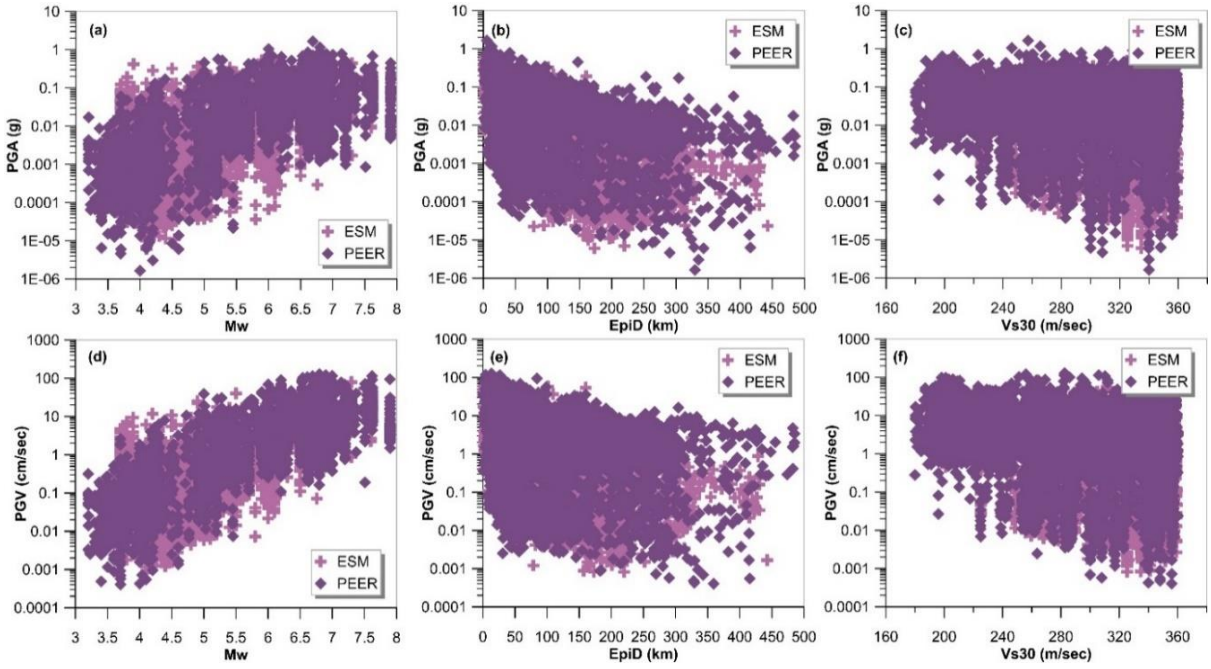

Fig. 5. Peak Ground Acceleration (PGA) and Peak Ground Velocity (PGV) plotted against: (a and d) moment magnitude (M_w), (b and e) epicentral distance (*EpiD*), and (c and f) average shear-wave velocity in the upper 30 meters (V_{s30})

Subplots (a) and (d) demonstrate a well-defined positive correlation between both PGA and PGV and moment magnitude (M_w), confirming the expected relationship where larger earthquakes produce stronger ground motions. The majority of the data cluster between M_w 4.5 and 6.5, with the PEER NGA-West2 dataset notably extending the coverage to higher magnitudes and more extreme PGV values, thereby enriching the analysis of high-energy events. Subplots (b) and (e) depict the characteristic attenuation of ground motion with increasing epicentral distance, a phenomenon driven by geometric spreading and anelastic attenuation. The consistent trends observed across both the ESM and PEER datasets validate the reliability of the combined dataset for analyzing distance-dependent ground motion behavior. In subplots (c) and (f), PGA and PGV exhibit more scattered and less pronounced correlations with V_{s30}, underscoring the complex influence of local site conditions. While higher V_{s30} values (typically indicative of stiffer rock sites) generally correspond to reduced amplification, the variability in the data highlights the significant role of other site-specific factors, such as basin effects and nonlinear soil response.

Collectively, these observations align well with established ground motion principles. The synergistic use of the ESM and PEER datasets strengthens the analysis by providing complementary coverage across different magnitude ranges and distances, thereby enhancing the robustness and generalizability of the findings.

3.1. Prediction Models

To develop a reliable prediction model for PGA and PGV on soft soil sites, a functional form was adopted based on the general model proposed by Kramer (1996) [10]. This formulation links key parameters influencing ground motion, such as moment magnitude (M_w), epicentral distance ($EpiD$), and site conditions characterized by the average shear wave velocity over the top 30 meters (V_{s30}). The chosen functional form closely reflects the physical mechanisms of ground motion generation and propagation, minimizing reliance on purely empirical adjustments. Following the log-normal distribution assumption for ground motion parameters, regression analyses were performed on the logarithmic values of PGA and PGV. This approach ensures a robust predictive model that accurately incorporates the effects of magnitude scaling, source distance attenuation, and site amplification, aligning with best practices established in seismic hazard analysis.

3.2. PGA Model for Soft Soil

Predictive relationships for parameters that decrease with distance—such as peak acceleration and peak velocity—are often referred to as attenuation relationships. Douglas (2019) [26] has summarized over 450 attenuation relationships for predicting PGA. Each model is best suited to conditions similar to those of the databases from which it was derived. Eq. (3) is commonly used to describe PGA attenuation [27–31]. In this study, we adopt this formula to represent PGA attenuation in soft soil sites. Typically, the constant b is positive and relates to seismic energy attenuation, while the constant c is negative, representing the effect of distance attenuation.

$$log(PGA) = a + b(M_w - 6) + c(M_w - 6)^2 + d \times log(R) + e(R) \quad (3)$$

In Eq. (3), *a, b, c, d*, and *e* are regression coefficients; PGA is the predicted peak ground acceleration expressed in units of g (where 1 g = 9.80665 m/s^2 = 980.665 cm/s^2); M denotes the source energy, represented by the moment magnitude M_w; R is the hypocentral distance to the recording site (in kilometers); and log refers to the base-10 logarithm. Table 2 presents the regression coefficients for the ESM and PEER databases individually, derived using nonlinear multiple regression analysis based on the Nonlinear Least Squares algorithm. Table 3 provides the corresponding model coefficients for the combined dataset, including their associated confidence intervals, using the same functional form as Eq. (3).

Table 2. Coefficients of the proposed PGA prediction model for PEER and ESM datasets

Coefficients	*a*	*B*	*c*	*d*	*e*	R^2	RMSE
PEER	0.6525	0.5704	-0.101600	-1.052	-0.002018	0.8663	0.3402
ESM	0.9484	0.6613	0.009506	-1.394	-0.001616	0.7632	0.4402
All data	0.8400	0.6349	-0.056670	-1.211	-0.001906	0.8354	0.3962

Table 3. Coefficients of the proposed PGA prediction model for combined dataset.

Coefficients	*A*	*b*	*c*	*d*	*e*
Combined database	0.8400	0.6349	-0.05667	-1.211	-0.001906
Confidence interval	0.7733; 0.9066	0.6232; 0.6466	-0.06407; -0.04927	-1.255; -1.167	-0.002112; -0.0017

Fig. 6 presents both the prediction surfaces and residual distributions for PGA models developed using three datasets: All (combined), PEER, and ESM. In subplots (a)–(c), the predicted Log(PGA) surfaces illustrate a consistent physical trend across all datasets: ground motions increase with magnitude and decrease with epicentral distance, reflecting attenuation effects. The scatter points show the actual data used for model fitting, and the surfaces indicate good alignment between observed and predicted values.

Subplots (d)–(f) visualize the residuals—differences between observed and predicted Log(PGA) values—for each dataset. In these plots a positive residual indicates under-prediction by the model and a negative residual indicates over-prediction by the model. In all three cases, the residuals are generally centered around zero with no evident systematic bias, indicating satisfactory model performance. However, the residual spread differs slightly among datasets: the PEER and ESM datasets (e, f) exhibit more compact residuals, potentially due to more homogeneous data characteristics or smaller sample sizes. In contrast, the All dataset (d) shows greater variability, likely due to combining data from diverse sources. These visualizations collectively validate the predictive strength of the developed models while also highlighting areas of potential refinement, especially for broader datasets.

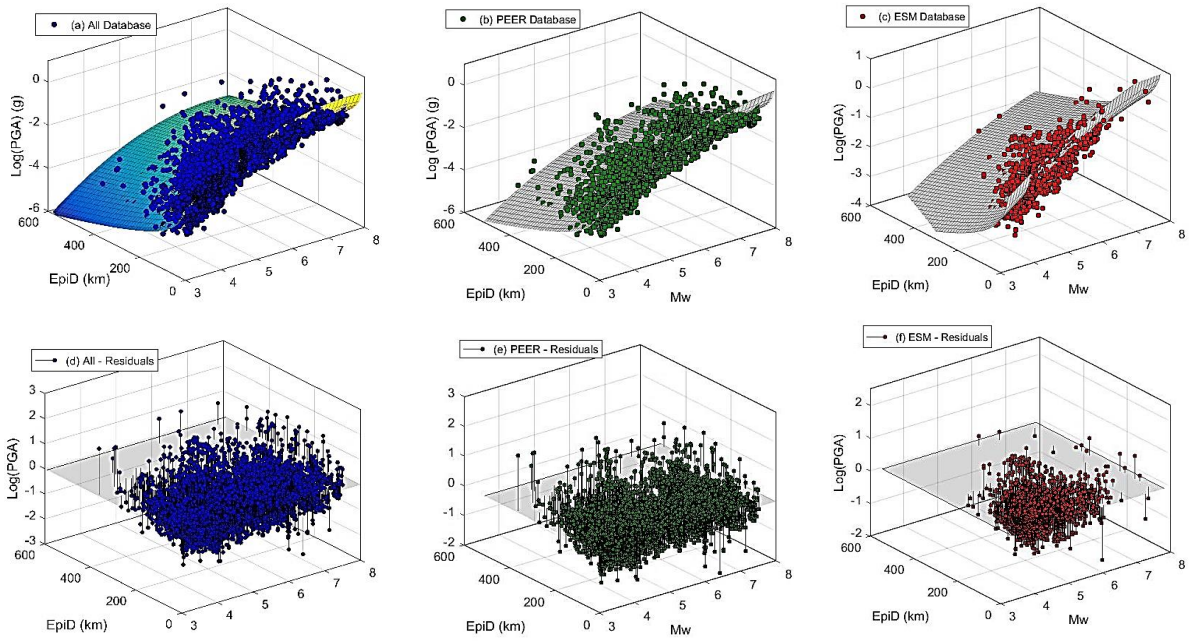

Fig. 6. (a–c) Three-dimensional views of the predicted PGA models for the All, PEER, and ESM datasets, respectively, as a function of *EpiD* and M_w. The surfaces represent the model fit to the observed data. (d–f) Corresponding residual plots for each dataset. Residuals are plotted in the same 3D space to evaluate the model's performance across magnitude and distance ranges

3.3. Assessment of the Proposed PGA Model

To assess whether the PGA model presented above, based on the employed data, accounts for behavior primarily influenced by M_w and *EpiD*, we have plotted the predicted PGA as a function of both parameters in the following figures. Fig. 7 presents the variation of Peak Ground Acceleration (PGA) as a function of epicentral distance (*EpiD*) for different earthquake magnitudes (M_w = 3.5, 4.5, 5.5, 6.5, and 7.5) in soft soil conditions. In all subplots, PGA decreases as the epicentral distance

increases, which is expected due to energy dissipation over distance. Higher magnitude earthquakes (M_w = 6.5, 7.5) show higher PGA values, especially at short distances.

The PEER and combined models seem to align closely, indicating that the PEER dataset follows the overall trend well. The ESM dataset (blue dashed line) generally predicts higher PGA values compared to PEER, particularly at shorter distances. For smaller magnitudes (M_w = 4.5, 5.5), differences between the models are relatively minor. For larger magnitudes (M_w = 6.5, 7.5), the divergence between ESM and PEER predictions becomes more noticeable, with ESM systematically predicting higher PGA.

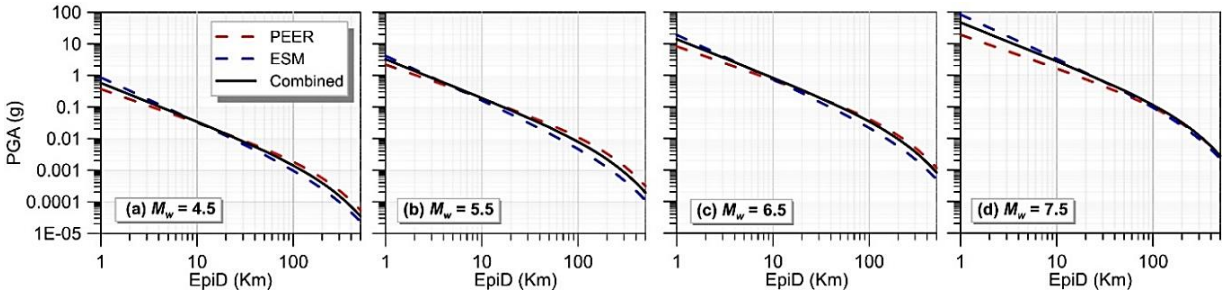

Fig. 7. Variation of PGA as a function of *EpiD* for different earthquake magnitudes (M_w = 3.5, 4.5, 5.5, 6.5, and 7.5) in soft soil conditions. The black continuous line represents the developed predictive model using the combined datasets

The Fig. 8 illustrates the variation of predicted Peak Ground Acceleration (PGA) with moment magnitude (M_w) for four source-to-site epicentral distances (*EpiD* = 10 km, 50 km, 100 km, and 150 km), based on empirical ground motion models calibrated using three datasets: the PEER and ESM strong-motion databases, and their combined compilation.

For all distance intervals, PGA increases systematically with M_w, consistent with source scaling behavior observed in empirical ground motion studies. A pronounced attenuation trend is evident with increasing epicentral distance, reflecting both geometric spreading and anelastic damping effects in crustal propagation paths. The ESM-derived model consistently yields higher PGA estimates across the magnitude range, particularly in the near field (e.g., *EpiD* = 10 km), potentially due to regional differences in site amplification, crustal attenuation, and event selection criteria.

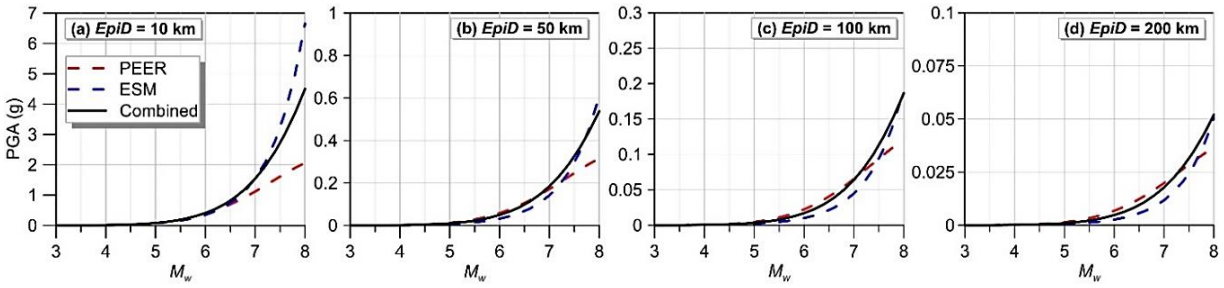

Fig. 8. Predicted Peak Ground Acceleration (PGA) as a function of moment magnitude (M_w) for four epicentral distances: (a) 10 km, (b) 50 km, (c) 100 km, and (d) 200 km. Ground motion prediction models were developed using the PEER (red dashed line) and ESM (blue dashed line) strong-motion databases, along with their combined dataset (black solid line)

In contrast, the PEER-based model predicts lower PGA values, particularly at shorter distances. The combined dataset generates intermediate predictions, capturing characteristics from both regions and offering a more generalized model. The reduced spread between models at greater distances suggests that far-field motions are less sensitive to localized site and source-region effects.

The ESM-based model yields higher PGA values, particularly in the near field, which may reflect stronger site amplification effects and regional attenuation characteristics. The PEER-based model provides lower estimates, while the combined model exhibits intermediate behavior, suggesting a balanced integration of source and path effects from both datasets. The convergence of predictions at larger distances indicates reduced sensitivity to local site and regional source characteristics in

the far field. The ESM dataset generally predicts higher PGA values, especially at shorter distances, whereas the PEER dataset aligns more closely with the overall model. At greater distances, the differences between models diminish, highlighting the dominant effect of attenuation on seismic ground motion.

A second comparison is conducted using actual data from each database. Fig. 9 presents Peak Ground Acceleration (PGA) values from the PEER dataset (blue triangles) and the ESM dataset (red triangles), alongside model-predicted PGA curves for different epicentral distances (Fig. 9a) and earthquake magnitudes (Fig. 9b) in soft soil conditions.

The proposed model accurately predicts PGA variations with both magnitude and distance, demonstrating strong alignment with observed values from the PEER dataset. As expected, shorter distances and higher magnitudes correspond to greater PGA values, while attenuation effects become more prominent at larger distances.

For the ESM dataset, the model effectively captures the overall trend of PGA variation. However, some recorded values exceed predictions, highlighting the complexity of seismic ground motion behavior in soft soil conditions and the potential influence of site-specific factors. Despite this variability, the model provides a reliable representation of attenuation trends and magnitude-dependent PGA variations.

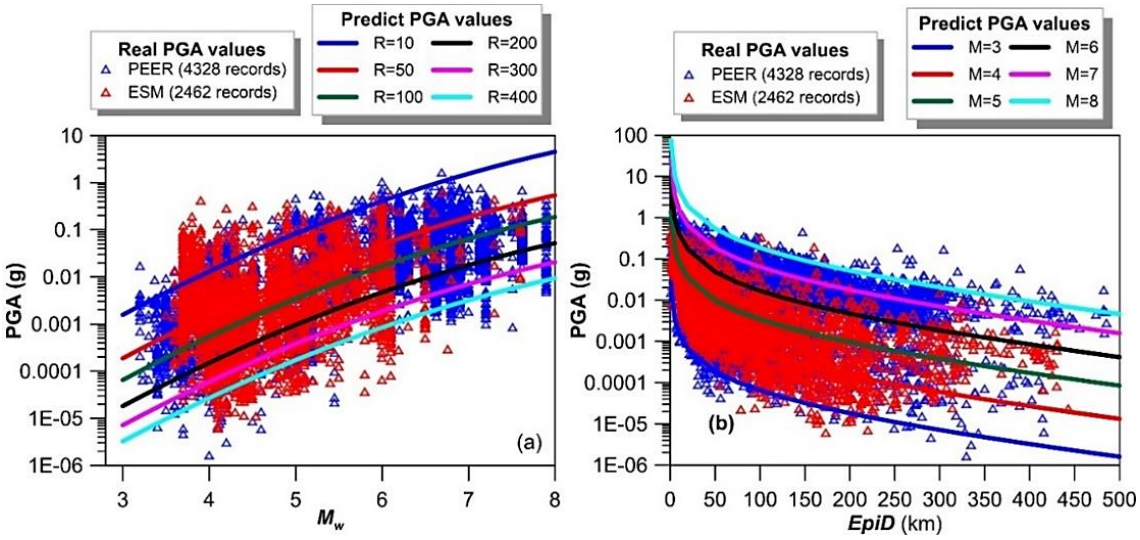

Fig. 9. Comparison of observed and predicted PGA values from the PEER (blue triangles) and ESM (red triangles) datasets. (a) PGA as a function of M_w for different *EpiD* and (b) PGA as a function of *EpiD* for different M_w

As the final validation, we conducted a comprehensive benchmarking analysis against established ground motion prediction equations (GMPEs) from the literature. Douglas (2017) [26] systematically reviewed over 450 PGA attenuation relationships, the majority of which employ regression-derived coefficients. For this comparative study, we selected representative models that: (1) incorporate site classification parameters, (2) demonstrate robust performance in previous validation studies, and (3) are widely adopted in engineering practice. This comparative framework enables rigorous evaluation of our soft soil-specific PGA model's predictive capabilities relative to conventional approaches.

In 1981, Campbell [32] developed an attenuation relationship using global data to estimate the average PGA at sites located within 50 km of the fault rupture during earthquakes with magnitudes ranging from 5.0 to 7.7. This model, represented by Eq. 1 in Table 4, was considered state-of-the-art at the time. Subsequently, Youngs et al. (1988) [33] used strong-motion records from rock sites during 60 earthquakes, along with numerical simulations for events with $M_w < 8$, to develop an attenuation relationship specific to subduction zones. Their proposed formula is given by Eq. 2 in Table 4.

In 1993, Boore et al. [28] introduced a more advanced model incorporating multiple terms. Their model was based on data from earthquakes with magnitudes ranging from 5.0 to 7.7 in western North America at distances of less than 100 km from the surface projection of the fault. The corresponding formula is presented in Eq. 3 in Table 4.

The next proposed comparison model is given by Akkar et al. (2014) [34], who introduced a new generation of ground-motion models derived from pan-European databases. Their formula, representing the latest advancements in ground-motion modeling, is provided in Eq. 4 in Table 4.

Another prediction model called as Campbell and Bozorgnia (2014) for the horizontal components of PGA and PGV, developed by the Pacific Earthquake Engineering Research Center (NGA-West2) team, was used for comparison with the established models [35]. This model, applicable for periods ranging from 0.01 to 10 s (Eq. 5 in Table 4), employs a complex functional form with nine terms. These terms account for various factors, including earthquake magnitude scaling, geometric attenuation, faulting style, hanging-wall effects, shallow site response, basin effects, hypocentral depth, rupture dip, and apparent anelastic attenuation

More recently, Zuccolo et al. (2017) [36] developed a model using data from 61 stations located on Eurocode 8 class B sites ($360 \leq V_{s30} < 800$ m/s), primarily from 33 stations within the Irpinia Seismic Network, supplemented by data from other networks. Although data were originally collected from sites of different classes, 93% of the accelerograms were from class B sites.

The final chosen model for comparison is given by Shiuly (2018) [37] proposed a global attenuation relationship for estimating PGA at rock sites, making it applicable to any region worldwide. He developed four relationships using multiple regression and an additional model based on Genetic Programming. The model is given by Eq. 7 in Table 4.

Table 4. Selected PGA models for comparison with the proposed model

N	Prediction Model	Ref.
(1)	$\ln(PGA)_g = -4.141 + 0.868M - 1.09\ln(R + 0.0606e^{0.7M})$	[32]
(2)	$\ln(PGA)_g = 19.16 + 1.045M_w - 4.738\ln(R + 205.5e^{0.0968M_w}) + 0.54Z_t$	[33]
(3)	$\log(PGA)_g = -0.038 + 0.216(M_w - 6) - 0.77\log(R) + 0.158G_B + 0.254G_C, with\ R = \sqrt{d^2 + 5.48^2}$	[28]
(4)	$\ln(PGA)_g = \ln[PGA_{REF}(M_w, R, SoF)] + \ln[S(V_{s30}, PGA_{REF})]$	[34]
(5)	$\ln(\mathrm{PGA}) = f_{mag} + f_{dis} + f_{flt} + f_{hang} + f_{site} + f_{sed} + f_{hyp} + f_{dip} + f_{atn}$	[35]
(6)	$\log(PGA)_{m/sec^2} = -2.1575 + 0.8359M - 1.969log\ (R)$	[36]
(7)	$\log(PGA) = 0.3646 + 0.4215(M - 6) - 0.01869(M - 6)^2 - 0.9707\log(R) - 0.0008(R)$	[37]

Where M is the magnitude and R is the closest distance to the fault rupture in kilometers. Zt is the focal depth, which takes a value of 0 for convergent events and 3 for divergent events. d is the closest distance to the surface projection of the fault in kilometers, and: GB = {0 for site class A, 1 for class B, and 0 for class C}, GC = {0 for site class A, 0 for class B, and 1 for class C}. Note that in all proposed relationship, PGA is expressed in terms of the decimal logarithm rather than the natural logarithm. Site classes are defined based on the average shear wave velocity in the top 30 meters of depth.

Fig. 10 systematically compares the performance of our proposed ground motion attenuation model (solid black line) against seven established prediction models (Table 4) across four characteristic earthquake magnitudes: (a) M_w = 4.5, (b) M_w = 5.5, (c) M_w = 6.5, and (d) M_w = 7.5. This comparative analysis spans the full range of engineering interest, from minor to major seismic events, evaluating model behavior through peak ground acceleration (PGA) attenuation curves plotted against epicentral distance.

The comparative analysis between proposed PGA model for soft soils (V_{S30} = 180–360 m/s) and seven established attenuation relationships (Fig. 10) reveals critical insights about ground motion prediction in vulnerable soil conditions:

For moderate-magnitude earthquakes (M_w 5.5–6.5), the proposed model aligns closely with Akkar et al. (2014) at intermediate distances (50–200 km). However, it diverges significantly from rock-

site model (Campbell 1981; Shiuly 2018) and Campbell and Bozorgnia (2014) model, which systematically underpredict PGA by 30–50% due to their neglect of soil amplification effects. This discrepancy is particularly pronounced in the 0.1–1.0 g range, where soft soil amplification is most critical for structural design. The results confirm that magnitude significantly influences PGA prediction accuracy in soft soils, with conventional models failing to capture the nonlinear response of these vulnerable sites.

The proposed model exhibits distinct distance attenuation behavior compared to existing relationships. At short distances (<100 km), it shows faster PGA attenuation than Boore et al. (1993) and Youngs et al. (1988), reflecting the enhanced energy dissipation typical of soft soils. Beyond 300 km, the predictions converge with Campbell (1981), validating the model's far-field behavior. This dual-phase attenuation pattern—rapid decay near the source followed by stable far-field trends—highlights the importance of distance-dependent terms tailored to soft soil mechanics, which are absent in most conventional models.

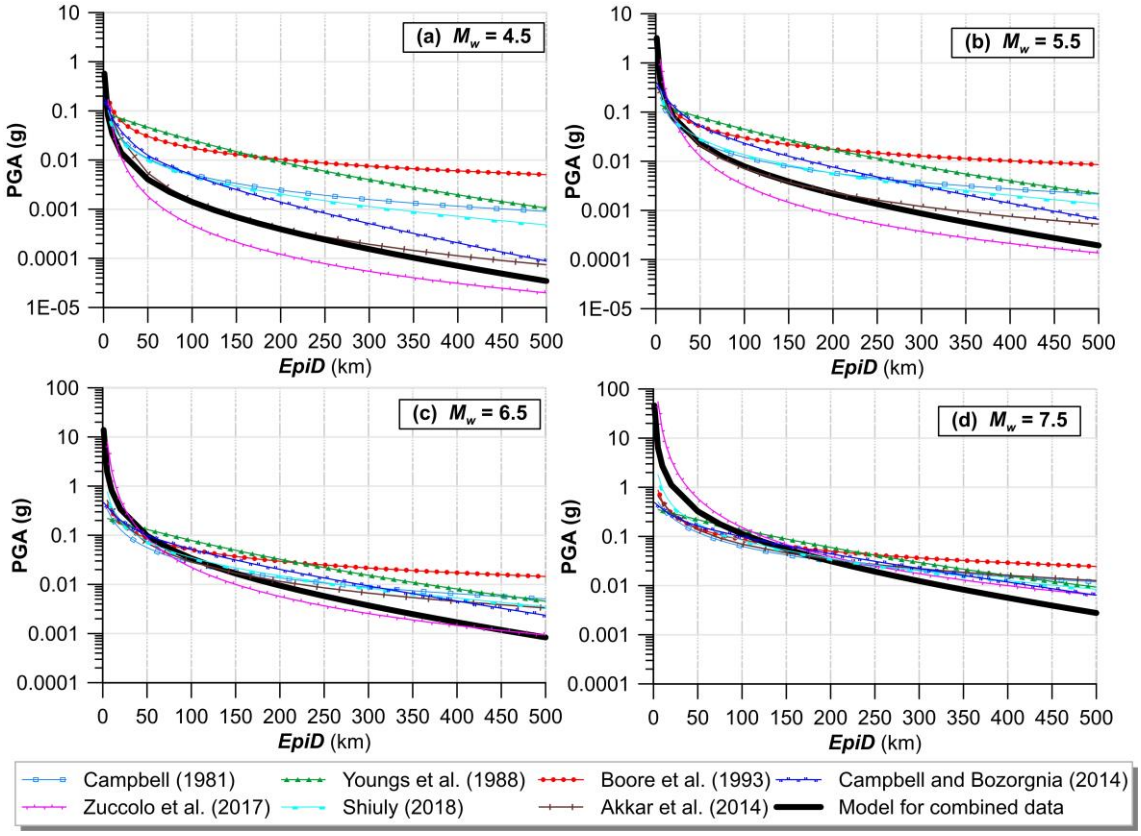

Fig. 10. Variation of PGA with epicentral distance for magnitudes M_w = 4.5, 5.5, 6.5, and 7.5, based on the proposed relationships for comparison

Rock-site models (Shiuly 2018; Zuccolo et al. 2017) consistently underpredict PGA across all magnitudes and distances, failing to capture the amplification peak observed at 50–150 km in soft soils. These models disregard key mechanisms such as impedance contrast and nonlinear soil behavior, leading to unsafe underestimations of ground motion. Their poor performance underscores the necessity of site-specific formulations for accurate hazard assessment in soft soil regions, particularly for infrastructure design where PGA thresholds are critical.

Region-specific models like Boore et al. (1993) (Western North America) and Akkar et al. (2014) (Europe) exhibit erratic behavior outside their calibration ranges, especially for $M_w \geq 7.5$. Their reliance on localized datasets introduces biases when applied to other tectonic settings or soil conditions. For instance, Boore et al. overpredicts PGA at intermediate distances in soft soils, while Akkar et al. shows inconsistent magnitude scaling. These limitations emphasize the need for globally representative data, as incorporated in the present model through the combined PEER and ESM databases.

The largest discrepancies between models occur in the 0.1–1.0 g PGA range, which is most relevant for seismic design. Existing models may underpredict PGA by up to 40% for $M_w \geq 6.5$, potentially leading to nonconservative designs. Our results demonstrate that soft soil amplification cannot be approximated using generic correction factors—a practice common in current standards. Instead, dedicated attenuation relationships, like the one proposed here, are essential to ensure safety and resilience in vulnerable regions.

The proposed model outperforms references by explicitly accounting for soft soil physics (V_{s30} 180–360 m/s) and combining global datasets (PEER + ESM). Its robust performance across magnitudes and distances stems from: (1) nonlinear soil response terms, (2) dual-phase attenuation formulation, and (3) calibration against modern strong-motion records. This advancement eliminates the need for ad-hoc corrections, providing a unified framework for PGA prediction in soft soils.

3.4. PGV Model for Soft Soil

Building upon the attenuation model developed by Joyner and Boore (1988) [38], we developed a PGV prediction model tailored for soft soil conditions. The model is expressed by the following equation:

$$log(PGV)_{[cm/sec]} = a + b(M_w - 6) + c(M_w - 6)^2 + d \times log\left(\sqrt{EpiD^2 + e^2}\right) \quad (4)$$

Where PGV denotes the peak ground velocity, and *EpiD* represents the epicentral distance (in kilometers). The model coefficients (*a, b, c, d, e*) were determined through nonlinear regression analysis and are summarized in Table 4 for each sub-dataset individually, and in Table 5 for the combined dataset. Each coefficient plays a distinct role in shaping the attenuation behavior of ground motion:

- Coefficient a represents a constant term that primarily influences the overall amplitude of the PGV. It sets the baseline level of the ground motion prediction across all distances and magnitudes.
- Coefficient b quantifies the influence of earthquake magnitude on PGV. A positive value, as observed in all datasets, indicates a direct correlation between magnitude and PGV, consistent with physical expectations.
- Coefficient c introduces a nonlinear adjustment—typically associated with a quadratic or higher-order magnitude term—allowing for finer calibration of the model, particularly at extreme magnitude values.
- Coefficient d governs the attenuation rate of PGV with respect to epicentral distance. The negative values observed across all datasets reflect the expected decay of ground motion intensity with increasing distance from the earthquake source.
- Coefficient e serves as an additional constant or intercept term, potentially accounting for site-specific effects or regional baseline shifts in PGV values.

Model performance was evaluated using the coefficient of determination (R^2) and the root mean square error (RMSE). The results show a strong model fit for the PEER database (R^2 = 0.9065, RMSE = 0.3154), indicating excellent predictive capability. The ESM database also yielded satisfactory results (R^2 = 0.8107, RMSE = 0.3783), albeit with slightly higher variability. The model calibrated on the combined dataset achieved a balanced performance (R^2 = 0.8862, RMSE = 0.3553), demonstrating its robustness across diverse records. The coefficient intervals provided in Table 6 represent the estimated 95% confidence bounds, highlighting the statistical reliability of the regression parameters.

Table 5. Coefficients of the proposed PGV prediction model given in Eq. (4) for PEER and ESM database

Coefficients	a	b	c	d	e	R2	RMSE
PEER	3.184	0.723	-0.09806	-0.7181	-11.97	0.9065	0.3154
ESM	3.062	0.8597	0.02912	-0.7620	-4.703	0.8107	0.3783

Table 6. Coefficients of the proposed PGV prediction model given in Eq. (4) for combined database

Coefficients	a	b	c	d	e	R2	RMSE
All data	3.147	0.7826	-0.05475	-0.738	-7.369	0.8862	0.3553
interval	3.084; 3.21	0.772; 0.7932	-0.06147; -0.04802	-0.7531; -0.7229	-8.51; -6.228		

Fig. 11 presents three-dimensional regression surfaces of the proposed PGV prediction model (Eq. 4), applied to different datasets: the combined dataset (Fig. 11a), the PEER database (Fig. 11b), and the ESM database (Fig. 11c). The plots illustrate the relationship between epicentral distance (*EpiD*), earthquake magnitude (M_w), and the logarithm of peak ground velocity (Log(PGV)). Each plot overlays the fitted regression surface onto the observed data points, enabling visual assessment of model performance across the parameter space.

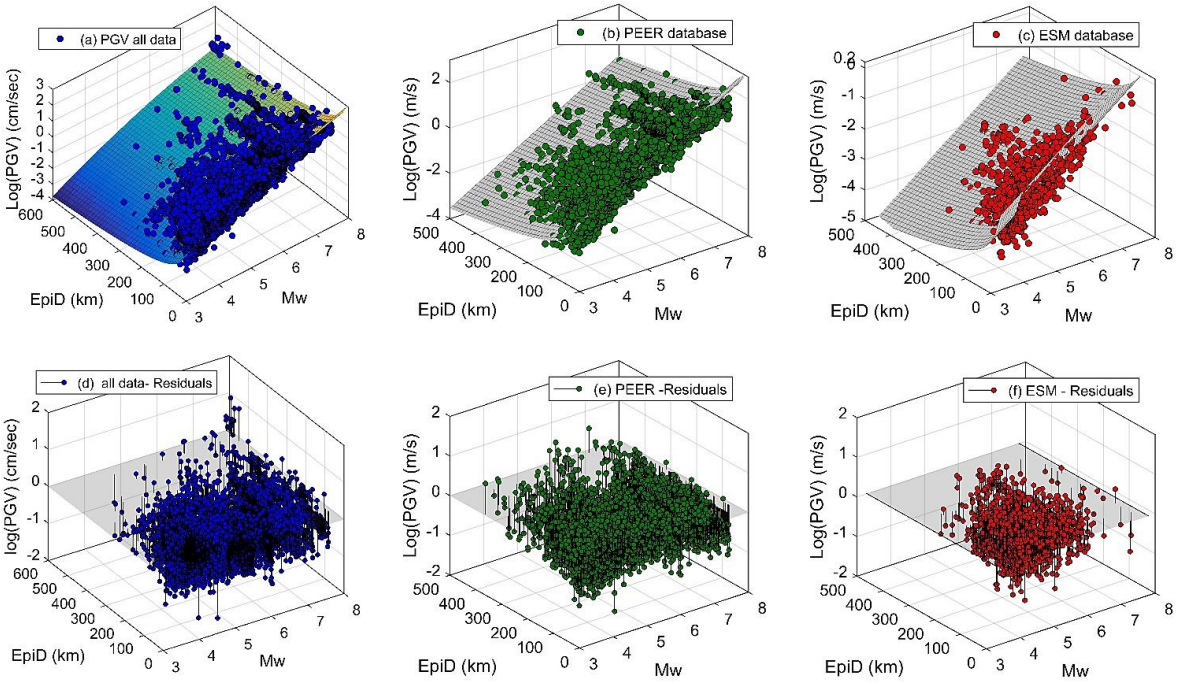

Fig. 11. (a–c) 3D views of the predicted PGV models for the All, PEER, and ESM datasets, respectively, as a function of *EpiD* and M_w. (d–f) Corresponding residual plots for each dataset

Fig. 11a demonstrates the model's fit to the entire dataset, showing a generally good agreement between observed and predicted values. The regression surface effectively captures the expected trend of increasing PGV with higher magnitudes and decreasing PGV with increasing epicentral distance. Fig. 11b focuses on the PEER dataset, which exhibits a dense and well-distributed set of observations. The regression surface closely aligns with the data, indicating strong model performance, consistent with the high R^2 value (0.9065) and low RMSE (0.3154) reported in Table 4. Fig. 11c displays the model performance for the ESM dataset, which shows a more dispersed pattern. While the general trend is captured, a slightly greater scatter around the regression surface is observed, which corresponds with the comparatively lower R^2 (0.8107) and higher RMSE (0.3783).

To further evaluate model accuracy, the bottom row of Fig. 11 (Figs. 11d-f) presents the residual distributions, defined as the difference between the observed and predicted Log(PGV) values. Fig. 11d shows the residuals for the combined dataset. The residuals are generally centered around zero, with no significant bias across the ranges of M_w or *EpiD*, indicating an overall balanced model. Fig. 10e displays residuals for the PEER dataset. The residuals are tightly clustered with minimal dispersion, further validating the high predictive quality of the model for this dataset. Fig. 11f presents residuals for the ESM dataset. Although the residuals remain centered near zero, a slightly broader spread is evident, especially at lower magnitudes, reflecting the higher variability in this

subset. Overall, the 3D regression surfaces and residual plots confirm that the proposed model reliably captures the attenuation trends of PGV for soft soil sites across different datasets, with particularly strong performance for the PEER records. The consistency in residual distributions supports the statistical robustness of the model across varying magnitudes and distances.

3.5. Assessment of the Proposed PGV Model

Fig. 12 presents the empirical prediction and observed data of Peak Ground Velocity (PGV) as functions of epicentral distance (*EpiD*) and moment magnitude (M_w), using ground motion records from the ESM (2462 records) and PEER (4328 records) databases. In subplot (a), PGV is plotted against *EpiD* for a range of fixed M_w values (3.5 to 8.0). The scatter points show the observed PGV values from both datasets, while the solid lines represent model predictions for the specified magnitudes. As expected, PGV shows a clear attenuation trend with increasing distance, and higher magnitudes produce significantly larger PGV values across all distances. In subplot (b), PGV is plotted against M_w for fixed epicentral distances (ranging from 10 km to 600 km). Here, PGV increases consistently with M_w, and the rate of increase is steeper at shorter distances. Model prediction curves closely follow the central tendency of the data, validating the model's ability to capture the magnitude-distance scaling relationship. The comparison highlights good agreement between the ESM and PEER datasets, reinforcing the robustness of the derived regression model across diverse regional data sources.

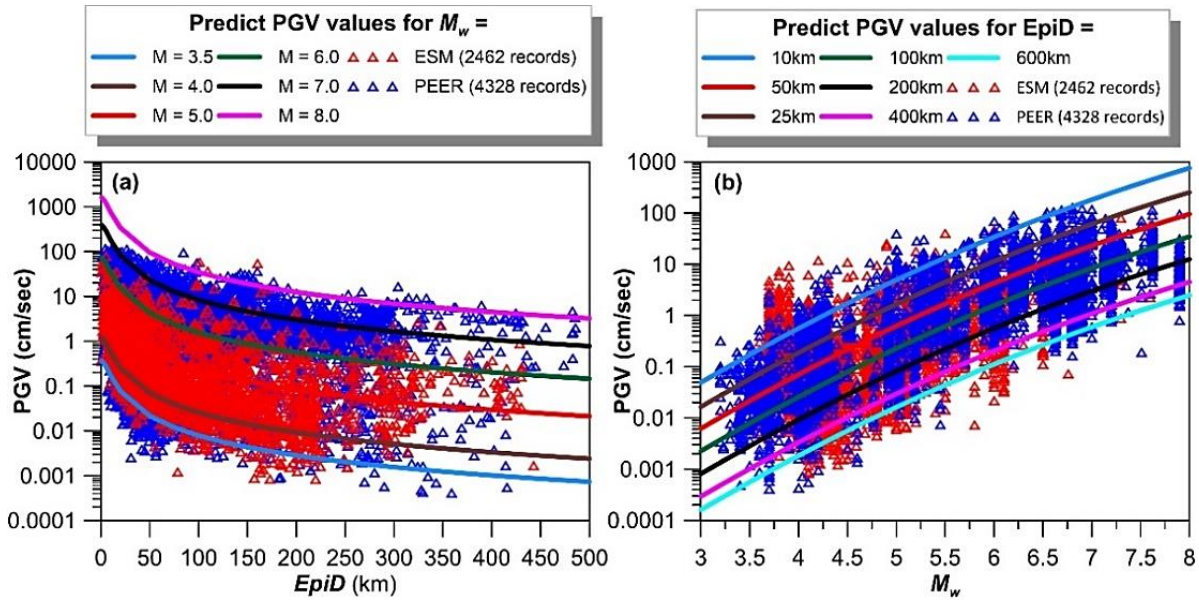

Fig. 12. Comparison of predicted and observed PGV values from the ESM (red triangles) and PEER (blue triangles) databases. (a) PGV versus *EpiD* for fixed M_w (3.5 to 8.0); (b) PGV versus M_w for fixed *EpiD* (10 km to 600 km). Solid lines represent regression model predictions

A second comparison is conducted using empirical models previously proposed in the literature. The first model, developed by Joyner and Boore (1988) [38], is presented in Equation (1) of Table 7. This attenuation relationship was derived from strong-motion recordings of earthquakes with moment magnitudes ranging from 5.0 to 7.7. However, it does not account for local site conditions, which may limit its applicability across diverse geological settings. The second comparison model, proposed by Massa et al. (2007) [39], was specifically developed for Central–Northern Italy, using a dataset of 2,126 ground-motion records. Their model incorporates site classification based on Eurocode 8, distinguishing between three categories: Class A (rock), Class B (stiff soil), and Class C (soft soil). The site condition parameter, S, is set to 1 for stiff or soft soil, and 0 otherwise. Additionally, the prediction model of Campbell and Bozorgnia (2014) [35], previously presented in Section 3.3, was utilized for comparison for the horizontal components of PGV. It should be noted that this model operates within specific parameter boundaries: moment magnitudes ranging from 3.3 to 8.5 for strike-slip faults, 8.0 for reverse faults, and 7.5 for normal faults; source-to-site distances limited to 300 km; shear wave velocities (V_{s30}) between 150-1500 m/s; and hypocentral

depths spanning 0-20 km [35]. A fourth comparison model was introduced by Akkar et al. (2014) [34], who developed a new generation of ground-motion prediction equations (GMPEs) based on a comprehensive pan-European strong-motion database. This model incorporates recent advancements in ground-motion modeling and is expressed in Eq. (4) of Table 1.

Finally, the model proposed by Tusa and Langer (2016) [40], based on an extensive dataset of seismic events from Mount Etna, Italy, was included. Their study considered 1,158 shallow and 1,957 deep events recorded across 91 stations, covering a magnitude range from 0.5 to 4.8 and epicentral distances up to 100 km. Their model accounts for both geological and volcanic site classifications, providing valuable insights for seismic hazard assessment in volcanic regions.

Table 7. Selected PGV models for comparison with the proposed model.

N	Prediction Model	Ref.
(1)	$\log(PGV)_{cm/s} = 2.09 + 0.49(M-6) - \log(R) - 0.002R + 0.17, with\ R = \sqrt{r_0{}^2 + 16}$	[38]
(2)	$\log(PGV)_{cm/s} = -4.197 + 0.856(M) - 1.727\log(R) + 0.178S$	[39]
(3)	$\ln(\mathrm{PGV}) = f_{mag} + f_{dis} + f_{flt} + f_{hang} + f_{site} + f_{sed} + f_{hyp} + f_{dip} + f_{atn}$	[35]
(4)	$\ln(PGV)_{cm/sec} = \ln[PGV_{REF}(M_w, R, SoF)] + \ln[S(V_{s30}, PGV_{REF})]$	[34]
(5)	$\ln(PGV)_{cm/sec} = -1.412 + 0.085M + 0.094M^2 + [-1.67 + 0.171(M-3.6)]\log\left(\sqrt{R_{ep}{}^2 + 3.056^2}\right) + 0.003\left(\sqrt{R_{ep}{}^2 + 3.056^2} - 1\right)$	[40]

Where M is the moment magnitude, and r_0 is the shortest distance (in kilometers) between the site and the vertical projection of the seismic fault rupture. *Rep* is the epicentral distance (km). S = 0 for Rock Site and 1 for Soil Site.

Fig. 13 presents a comparative analysis between the proposed PGV prediction model for soft soil sites and several established models from the literature given in Table 7. The comparison of PGV values is performed for four representative moment magnitudes: M_w = 4.5, 5.5, 6.5, and 7.5 against epicentral distance (*EpiD*) up to 400 km.

The Joyner & Boore (1988) model, while foundational for ground motion prediction, exhibits significant underestimation of PGV for soft soil sites across all magnitudes (Fig. 13). This discrepancy is most pronounced for $M_w \geq 5.5$, where the model underpredicts PGV by 40–60% at distances <100 km. The deviation stems from the model's lack of site-specific terms (e.g., V_{s30}), rendering it unsuitable for soft soil applications. These results underscore a critical gap in early attenuation relationships: their inability to account for soil amplification effects, which are particularly severe in loose, saturated deposits. Consequently, using such models for seismic hazard assessment in soft soil regions may lead to nonconservative designs, increasing vulnerability to infrastructure damage.

The Campbell and Bozorgnia (2014) and Akkar et al. (2014) models show region-dependent biases when applied to soft soils. Despite its comprehensive framework, Campbell and Bozorgnia (2014) overpredicts PGV for moderate magnitudes (M_w = 4.5–5.5), but aligns better for $M_w \geq 6.5$, likely due to its calibration with California-specific basin effects. Conversely, Akkar et al. (2014) performs well for M_w = 5.5–6.5 but diverges at M_w = 7.5, reflecting limitations of its pan-European dataset. Both models struggle with very soft soils (V_{s30} < 250 m/s), as their functional forms prioritize broader applicability over localized nonlinear effects. This highlights a key challenge in ground motion modeling: balancing regional generality with site-specific accuracy, particularly for high-risk soft soil zones.

Tusa & Langer (2016)'s model, developed for volcanic environments ($M_w \leq 4.8$, *EpiD* ≤ 100 km), performs poorly in this comparison (Fig. 13). Its predictions deviate substantially for $M_w \geq 5.5$ and distances >100 km, as it neglects crustal earthquake dynamics and deep soil amplification. This mismatch emphasizes the dangers of adopting region-specific models outside their intended context, particularly when assessing soft soil response to larger, non-volcanic events. Engineers

working in tectonic settings with mixed seismicity (e.g., Japan, Central America) should avoid such models unless volcanic hazards dominate.

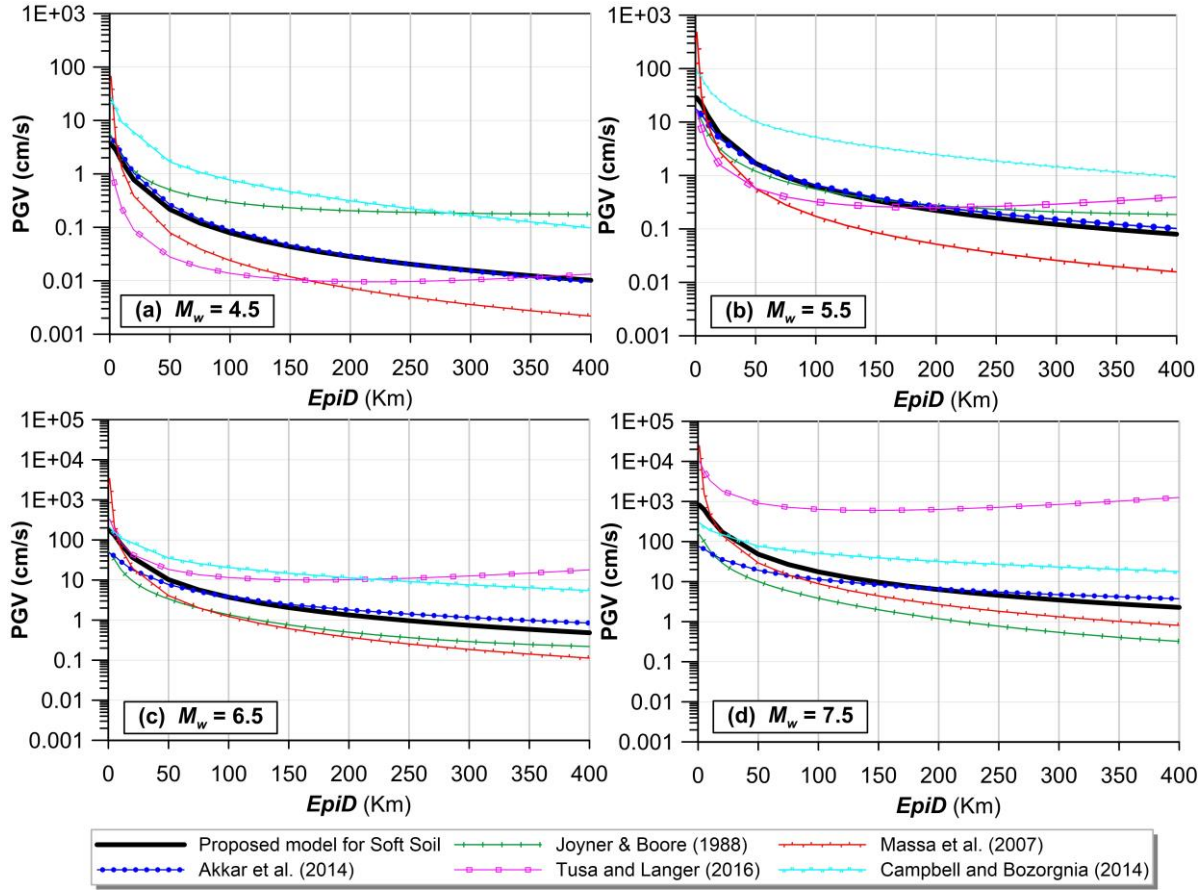

Fig. 13. Comparison of the proposed PGV prediction model for soft soil sites (black line) with established models from the literature: Joyner & Boore (1988), NGA-West2 (2014), Akkar et al. (2014), Massa et al. (2007), and Tusa & Langer (2016). PGV is plotted as a function of *EpiD* for four different M_w: (a) 4.5, (b) 5.5, (c) 6.5, and (d) 7.5

The proposed model shows superior agreement with observed PGV trends across all magnitudes and distances (Fig. 13), particularly in the 20–300 km range most critical for infrastructure design. Its enhanced accuracy derives from three key innovations: (1) explicit V_{s30}-dependence (180–360 m/s) to capture nonlinear soil behavior, (2) calibration with global datasets (PEER + ESM) to minimize regional biases, and (3) physics-based attenuation terms that account for dual-phase decay (rapid near-field vs. stable far-field shaking) in soft soils. Notably, for M_w = 7.5 events, the model predicts PGV values 20–30% higher than Campbell and Bozorgnia (2014) at 50–150 km distances, accurately reflecting empirical observations of prolonged shaking in soft basins. This improvement has direct implications for assessing liquefaction risk and designing long-period structures, where PGV serves as a critical demand parameter.

This comprehensive evaluation demonstrates that conventional ground motion models—whether rock-site-based (e.g., Joyner & Boore 1988), regionally constrained (e.g., Akkar et al. 2014), or volcanically calibrated (Tusa & Langer 2016)—exhibit systematic limitations in predicting PGV for soft soil conditions. The proposed model overcomes these shortcomings through its physics-based formulation incorporating V_{s30}-dependent nonlinearity (180-360 m/s), global dataset integration (PEER+ESM), and dual-phase attenuation behavior. Quantitative comparisons reveal its superior performance, particularly for critical scenarios (M_w ≥6.5, *EpiD* = 50-300 km), where it resolves 20-50% underprediction by existing models. These findings underscore the necessity of adopting site-specific attenuation relationships in seismic design codes, particularly for vulnerable soft soil regions where conventional approaches may compromise structural safety through unconservative predictions. The model's validated accuracy across magnitudes (4.5-7.5) and

distances (0-500 km) provides engineers with a robust tool for realistic hazard assessment in high-risk environments.

4. Conclusion

This study presents the development of a predictive model for Peak Ground Acceleration (PGA) and Peak Ground Velocity (PGV) in soft soil conditions, emphasizing the significant role of soft soil in amplifying seismic waves and increasing structural vulnerability during earthquakes.

The predictive model, based on nonlinear regression analysis, integrates key predictor variables, including moment magnitude (M_w), epicentral distance ($EpiD$), and average shear wave velocity over the top 30 meters (V_{s30}). Analyzing an extensive dataset of over 6790 ground motion records from 875 earthquakes (sourced from the PEER and ESM databases), the study underscores the importance of site classification, particularly shear wave velocity (V_{s30}), in assessing ground motion characteristics.

Key Conclusions:

- The proposed models effectively capture the influence of earthquake magnitude and epicentral distance on seismic ground motion in soft soil conditions, showing strong agreement with observed data from the PEER and ESM datasets.
- For PGA, the model accurately describes attenuation trends and magnitude-dependent variations. While the ESM dataset predicts slightly higher PGA values, especially at short distances, the model aligns well with established attenuation relationships (e.g., Campbell, 1981; Youngs et al., 1988; Boore et al., 1993). The findings highlight the importance of site-specific datasets for seismic hazard assessments in soft soil environments, given the faster attenuation observed at short distances.
- Fig. 10 demonstrates that soft soil response exhibits strong dependencies on both earthquake magnitude (M_w) and source-to-site distance ($EpiD$), necessitating specialized modeling approaches. Traditional models developed for rock sites or limited regional conditions are inadequate for these high-risk areas, highlighting the urgent need to adopt soil-specific attenuation relationships in seismic codes and hazard assessments. The proposed model addresses this gap, providing reliable predictions for critical engineering applications.
- For PGV, results confirm that earthquake magnitude has a stronger influence than distance, with PGV values increasing significantly as magnitude grows. The proposed model predicts higher PGV values at short distances than the widely used Joyner and Boore (1988) model, emphasizing the role of local soil amplification effects.
- Overall, the findings validate the reliability of the proposed models for seismic hazard analysis in soft soil regions. Comparisons with existing models reinforce the necessity of site-specific ground motion prediction equations (GMPEs) for accurate seismic risk assessments, particularly in areas where soft soil conditions amplify seismic waves.

To further enhance the accuracy and applicability of these predictive models, future research should:

- Incorporate additional geotechnical parameters for improved ground motion prediction.
- Develop refined earthquake-resistant design strategies, ultimately enhancing structural resilience in seismically active areas with soft soil conditions.
- Expand the database to include V_{s30} < 180 m/s (very soft soils).
- Incorporate basin depth effects, which may further modulate long-period motions.

The ground motion prediction equations (GMPEs) developed in this study provide a critical foundation for site-specific seismic hazard assessment in soft soils. However, to fully leverage these results for engineering applications, future research should investigate the role of soil-structure interaction (SSI) in modulating the seismic response of structures subjected to the predicted PGA and PGV. Such work would enhance the practical utility of these GMPEs by bridging the gap between ground motion prediction and performance-based seismic design, particularly for infrastructure in soft-soil regions.

Acknowledgement

The contributions of the PEER and ESM working group are acknowledged to provide earthquake database of this study.

References

[1] Vuran E, Serhatoğlu C, Timurağaoğlu MÖ, Smyrou E, Bal İE, Livaoğlu R. Damage observations of RC buildings from 2023 Kahramanmaraş earthquake sequence and discussion on the seismic code regulations. Bull Earthq Eng 2025;23:1153–82. https://doi.org/10.1007/s10518-023-01843-3
[2] Yao X, Wu B. Progress in Seismic Isolation Technology Research in Soft Soil Sites: A Review. Buildings 2024;14:3198. https://doi.org/10.3390/buildings14103198
[3] Shi F, Lin Z, Li Q, Ozbulut OE, He Z, Zhou Y. Design, manufacturing, and testing of a hybrid self-centering brace for seismic resilience of buildings. Earthq Eng Struct Dyn 2023;52:1381–402. https://doi.org/10.1002/eqe.3821
[4] Gue SS, Gue CS. Geotechnical Challenges On Soft Ground. J Civ Eng Sci Technol 2022;13:84–96. https://doi.org/10.33736/jcest.4760.2022.
[5] Roy M. Foundation on Soft and Filled-Up Soil. Geotech. Found. Eng. Pract. Ind. Proj., Singapore: Springer Nature Singapore; 2024, p. 93–103. https://doi.org/10.1007/978-981-99-7906-6_6
[6] Aouari I, Benahmed B, Palanci M, Aidaoui L. Empirical Model for the Prediction of Ground Motion Duration on Soft Soils. Indian Geotech J 2024;54:421–40. https://doi.org/10.1007/s40098-023-00778-5
[7] Almansa FL, Weng D, Li T, Alfarah B. Suitability of Seismic Isolation for Buildings Founded on Soft Soil. Case Study of a RC Building in Shanghai. Buildings 2020;10:241. https://doi.org/10.3390/buildings10120241
[8] Dagen W, Li T, López-Almansa F. Nonlinear Time-History Analysis of A Base-Isolated RC Building in Shanghai Founded on Soft Soil. 16th World Conf. Earthq. Eng., Santiago Chile: 2017, p. 2634.
[9] Griffiths SC, Cox BR, Rathje EM. Challenges associated with site response analyses for soft soils subjected to high-intensity input ground motions. Soil Dyn Earthq Eng 2016;85:1–10. https://doi.org/10.1016/j.soildyn.2016.03.008
[10] Kramer SL, Stewart JP. Geotechnical Earthquake Engineering. 2nd Editio. Boca Raton: CRC Press; 2024. https://doi.org/10.1201/9781003512011
[11] Giardini, D., Grünthal, G., Shedlock, K. M. and Zhang P. No TitleThe GSHAP Global Seismic Hazard Map. In: Academic Press A, editor. Int. Handb. Earthq. Eng. Seismol. Internatio, Amsterdam: 2003, p. 1233–9.
[12] Chasanah U, Handoyo E, Rahmawati NN, Musfiana M. Mapping Risk Level Based on Peak Ground Acceleration (PGA) and Earthquake Intensity Using Multievent Earthquake Data in Malang Regency, East Java, Indonesia. J ILMU Fis | Univ ANDALAS 2022;14:64–72. https://doi.org/10.25077/jif.14.1.64-72.2022
[13] Basid A, Rusli R, Purwandari P. Mapping The Risk Level of Earthquake Damage in Central Java Based on Data From PGA, PD and HDI. J Pendidik Fis Dan Keilmuan 2022;7:130. https://doi.org/10.25273/jpfk.v7i2.12078
[14] Akkar S, Özen Ö. Effect of peak ground velocity on deformation demands for SDOF systems. Earthq Eng Struct Dyn 2005;34:1551–71. https://doi.org/10.1002/eqe.492
[15] Hunter JA, Motazedian D, Crow HL, Brooks GR, Miller RD, Pugin AJ-M, et al. Near-Surface Shear-Wave Velocity Measurements for Soft-Soil Earthquake-Hazard Assessment: Some Canadian Mapping Examples. Adv. Near-surface Seismol. Ground-penetrating Radar, Society of Exploration Geophysicists, American Geophysical Union, Environmental and Engineering Geophysical Society; 2010, p. 339–59. https://doi.org/10.1190/1.9781560802259.ch21
[16] FEMA P-58. Seismic Performance Assessment of Buildings. Federal Em. 2018.
[17] KAWASHIMA K, UNJOH S. The Damage of Highway Bridges in The 1995 Hyogo-Ken Nanbu Earthquake and Its Impact on Japanese Seismic Design. J Earthq Eng 1997;1:505–41. https://doi.org/10.1080/13632469708962376
[18] Course S. Seismic Design of Buried Pipelines. University at Buffalo, State University of New York: 2012.
[19] Timothy D. Ancheta, Robert B. Darragh, Jonathan P. Stewart, Emel Seyhan, Walter J. Silva, Brian S.J. Chiou, Katie E. Wooddell, Robert W. Graves, Albert R. Kottke, David M. Boore, Tadahiro Kishida and JLD. PEER NGA-West2 Database. 2013.
[20] Luzi L, Lanzano G, Felicetta C, D'Amico MC, Russo E, Sgobba S, et al. Engineering Strong Motion Database (ESM), version 2.0 2020. https://doi.org/10.13127/ESM.2.
[21] Council IC, International Code Council. International Building Code. 5th ed. ICC; 2006.
[22] BSSC. 2000 NEHRP recommended provisions for seismic regulations for new buildings and other structures. FEMA-368 Part 1 Dev Fed Emerg Manag Agency, Washington, DC 2001.

[23] Eurocode-8. Eurocode 8: Design of structures for earthquake resistance - Part 1 : General rules, seismic actions and rules for buildings. Brussels, Belgium: European Committee for Standardization; 2004.
[24] UBC. Uniform Building Code. California, USA: International Conference of Building Officials; 1997.
[25] RPA. Régles Parasismiques Algériennes RPA 2024. Algeria: 2024.
[26] Douglas J. Ground motion prediction equations 1964-2018. vol. 69. 75 Montrose Street, Glasgow, United Kingdom: 2019. https://doi.org/10.1111/j.1651-2227.1980.tb07069.x
[27] Abrahamson NA, Silva WJ. Empirical Response Spectral Attenuation Relations for Shallow Crustal Earthquakes. Seismol Res Lett 1997;68:94–127. https://doi.org/10.1785/gssrl.68.1.94
[28] Boore DM, Joyner WB, Fumal TE. Equations for Estimating Horizontal Response Spectra and Peak Acceleration from Western North American Earthquakes: A Summary of Recent Work. Seismol Res Lett 1997;68:128–53. https://doi.org/10.1785/gssrl.68.1.128
[29] Campbell KW. Empirical Near-Source Attenuation Relationships for Horizontal and Vertical Components of Peak Ground Acceleration, Peak Ground Velocity, and Pseudo-Absolute Acceleration Response Spectra. Seismol Res Lett 1997;68:154–79. https://doi.org/10.1785/gssrl.68.1.154
[30] Chiou B-J, Youngs RR. An NGA Model for the Average Horizontal Component of Peak Ground Motion and Response Spectra. Earthq Spectra 2008;24:173–215. https://doi.org/10.1193/1.2894832
[31] Campbell KW. Updated Near-Source Ground-Motion (Attenuation) Relations for the Horizontal and Vertical Components of Peak Ground Acceleration and Acceleration Response Spectra. Bull Seismol Soc Am 2004;94:2417. https://doi.org/10.1785/0120040147
[32] Campbell K. Near-source attenuation of peak horizontal acceleration. Bull Seismol Soc Am 1981;71:2039–70.
[33] Youngs RR, Day SM, Stevens JL. Near field ground motions on rock for large subduction earthquakes. Earthq. Eng. Soil Dyn. II, vol. ASCE, 1988, p. 445–62
[34] Akkar S, Sandıkkaya MA, Bommer JJ. Empirical ground-motion models for point- and extended-source crustal earthquake scenarios in Europe and the Middle East. Bull Earthq Eng 2014;12:359–87. https://doi.org/10.1007/s10518-013-9461-4
[35] Campbell KW, Bozorgnia Y. NGA-West2 Campbell-Bozorgnia Ground Motion Model for the Horizontal Components of PGA , PGV , Response Spectra for Periods Ranging from 0.01 to 10 sec. Berkeley: 2013.
[36] Zuccolo E, Bozzoni F, Lai CG. Regional Low-Magnitude GMPE to Estimate Spectral Accelerations for Earthquake Early Warning Applications in Southern Italy. Seismol Res Lett 2017;88:61–71. https://doi.org/10.1785/0220160038
[37] Shiuly A. Global Attenuation Relationship for Estimating Peak Ground Acceleration. J Geol Soc India 2018;92:54–8. https://doi.org/10.1007/s12594-018-0952-4
[38] Joyner WB, Boore DM. Measurement, characterization, and prediction of strong ground motion. Earthq. Eng. Soil Dyn. II, Proc. Am. Soc. Civ. Eng. Geotech. Eng. Div. Spec. Conf., June 27–30, 1988, Park City, Utah, 1988, p. 43–102.
[39] Massa M, Marzorati S, D'Alema E, Di Giacomo D, Augliera P. Site Classification Assessment for Estimating Empirical Attenuation Relationships for Central-Northern Italy Earthquakes. J Earthq Eng 2007;11:943–67. https://doi.org/10.1080/13632460701232675
[40] Tusa G, Langer H. Prediction of ground motion parameters for the volcanic area of Mount Etna. J Seismol 2016;20:1–42. https://doi.org/10.1007/s10950-015-9508-x